

Field dependent effective masses in YbAl_3

T. Ebihara,¹ A. L. Cornelius,² J. M. Lawrence,³ S. Uji,⁴ and N. Harrison⁵

¹*Shizuoka University, Shizuoka 422-8529, Japan*

²*University of Nevada, Las Vegas, NV 89154*

³*University of California, Irvine CA 92697**

⁴*National Institute for Materials Science, Tsukuba 305-0003, Japan*

⁵*National High Magnetic Field Laboratory, Los Alamos NM 87545*

(Dated: March 10, 2019)

Abstract

We show for the intermediate valence compound YbAl_3 that the high field ($40 \lesssim B \lesssim 60\text{T}$) effective masses measured by the de Haas-van Alphen experiment for field along the $\langle 111 \rangle$ direction are smaller by approximately a factor of two than the low field masses. The field $B^* \sim 40\text{T}$ for this reduction is much smaller than the Kondo field $B_K \sim k_B T_K / \mu_B$ ($T_K \sim 670\text{K}$) but is comparable to the field $k_B T_{coh} / \mu_B$ where $T_{coh} \sim 40\text{K}$ is the temperature for the onset of Fermi liquid coherence. This suggests that the field scale B^* does not arise from $4f$ polarization but is connected with the removal of the anomalies that are known to occur in the Fermi liquid state of this compound.

PACS numbers: 75.30.Mb 75.20.Hr 71.27.+a 71.28.+d 61.10.Ht

The de Haas-van Alphen (dHvA) frequencies measured for nonmagnetic intermediate valence (IV) compounds such as CeSn_3 are generally in good agreement with the predictions of the LDA band theory that treats the $4f$ electron as itinerant[1]. While the LDA thus appears to give the geometry of the Fermi surface correctly, it seriously underestimates the large measured effective masses that arise in these strongly correlated systems. For CeSn_3 some of this disagreement can be remedied by use of the LDA+U approach[2].

For the IV compound YbAl_3 the LDA[3] fails to reproduce the measured Fermi surface. This failure is connected to the LDA prediction that the Yb $4f$ level is fully occupied ($4f^{14}$ or divalent Yb). Experiments[4] indicate nonintegral valence of the Yb ($4f^{14-n_f}$ with $n_f = 0.75$). Excellent agreement with the experimental dHvA frequencies[3] of YbAl_3 has been obtained in an LDA treatment where the energy of the $4f$ level is constrained in such a way as to permit nonintegral $4f$ occupation. The divalence that is incorrectly predicted by the LDA for other Yb compounds has also been remedied[5] by use of LDA+U; clearly the correlations affect the $4f$ level position as well as the effective masses.

For heavy fermion compounds with small Kondo temperatures, the application of a magnetic field larger than the Kondo field $B_K \sim k_B T_K / \mu_B$ is known to cause a large reduction in the measured effective masses[6]. This finds a natural explanation in the theory of a Kondo impurity[7] or of the Anderson lattice[8]: when the Zeeman splitting becomes larger than the Kondo temperature, the $4f$ level polarizes; the resulting reduction of the spin degeneracy inhibits the Kondo interaction that is responsible for the large effective masses. In this paper we show that the effective masses of key branches of the Fermi surface of YbAl_3 reduce by approximately a factor of two in magnetic fields of order $B^* = 40\text{T}$. A field of this magnitude is substantially smaller than the Kondo field $B_K \sim k_B T_K / \mu_B$ for this compound ($T_K = 670\text{K}$ [4]) and hence the transition cannot arise from $4f$ polarization. The field energy $\mu_B B^*$ does, however, correspond to the low energy scale $k_B T_{coh}$ ($T_{coh} \sim 40\text{K}$) for the onset of Fermi liquid coherence in YbAl_3 [3, 4]. We argue that the reduction of the effective mass is connected with the removal of the anomalous behavior[4] that occurs for $T < T_{coh}$ in this compound.

Single crystals of YbAl_3 were grown by the self-flux method, with excess aluminum[3]. The crystals were aligned using x-ray diffraction and reduced to the appropriate dimensions using a spark cutter followed by etching in acid solutions. The low-field (13-17T) and intermediate field (17-19.5T) dHvA measurements were performed using the field-modulation

technique at the National Institute for Materials Science in Tsukuba. The low field measurements allowed for measurement as a function of field angle relative to the high symmetry directions, and were performed using a dilution refrigerator with a lower temperature limit of 0.05K. The intermediate field measurements were performed at fixed angle using a He-3 refrigerator. The high field ($B \leq 57\text{T}$) dHvA signal was measured using the pulsed-field technique with counter-wound highly compensated pickup coils in the 60T short-pulse magnet at the National High Magnetic Field Laboratory in Los Alamos. The field angle was fixed for each sample, and the temperature was regulated between 0.5-1.5K using a He-3 refrigerator.

The dHvA frequencies for the low-field measurements are shown in Fig. 1. These reproduce the older work[3] with one nearly spherical high mass ($23\text{-}29m_e$) branch, denoted β , and several branches that are confined to the vicinity of particular field directions. The frequencies for intermediate field are essentially unchanged from those at low field. In Fig. 2a we show the fast Fourier transform (FFT) of the dHvA signal at high field ($45 < B < 55\text{T}$) at 0.84K and for field along the $\langle 111 \rangle$ direction. Four peaks are resolved, which correspond in frequency to the α , β , ϵ and η branches observed at low field[3]. The high field frequencies are equal, within a few percent, to those observed at low field (Fig. 1) with the exception of the frequency of the β branch, which is 25% larger than at low field.

We analyzed the high field measurements for each field range and temperature by fitting each FFT peak to the sum of a Gaussian and a second-order polynomial background function. We fit the Gaussian amplitudes to the function

$$A(B, T) \propto \left(\frac{F^2 T}{B^{5/2}} \right) \left(\frac{\partial B}{\partial t} \right) \frac{\exp[14.7m^*T_D/B]}{\sinh[14.7m^*T/B]} \quad (1)$$

where F is the dHvA frequency, m^* is the effective mass and T_D is the Dingle temperature. This formula is appropriate for pulsed field data[6]; a related expression appropriate for d.c. fields was used for the low and intermediate field data. By fitting at fixed field as a function of temperature we determined the effective mass for each branch and field range. Examples for the α and β branches are shown in Fig. 2b. By fitting at fixed temperature as a function of field, we determine the Dingle temperature (Fig. 2c).

The masses determined from this analysis are plotted as a function of field in Fig. 3. The plot includes the low and intermediate field values, and data from two different samples for each field orientation at high field. The scatter at high field gives a good indication of both

the reproducibility and the statistical error. Our key result is that the masses of the α and β branches for field along the $\langle 111 \rangle$ direction decrease by approximately a factor of two above 40T. Somewhat smaller reductions are observed for the η and ϵ branches. For field along the $\langle 100 \rangle$ direction there is a more modest decrease of the γ mass and the mass of the δ branch appears to *increase* with field.

We did not observe a dHvA signal for the β branch for field along either the $\langle 100 \rangle$ or the $\langle 110 \rangle$ directions. The low field masses for this branch for these directions are 28.9 and $26.3m_e$ respectively. From Equation 1 it is clear that large masses suppress the dHvA amplitude except at the lowest temperatures. In the pulsed field measurement, using a He-3 refrigerator, self-heating due to eddy currents limited our measurements to $T > 0.5\text{K}$. In this situation, it is very difficult to detect dHvA signals for branches with m^* much greater than $15m_e$. Our data is thus consistent with a reduction of the mass of the β branch for field in these directions, with a lower limit on the high field mass of order $15m_e$.

For similar reasons it was difficult to observe dHvA signals for the high mass branches for fields below about 35T. The field B^* for the transition to reduced masses is constrained by the dHvA data (Fig. 3) to lie somewhere in the interval $20 < B^* < 45\text{T}$. The susceptibility (Fig. 3, inset) is constant up to 40T, and decreases at higher field, suggesting that $B^* \sim 40\text{T}$. The field dependence of the amplitude of the α branch fits the predicted Dingle curve for $B > 38\text{T}$ (Fig. 2c) which also suggests a transition field of this magnitude.

We have recently shown[3, 4] that $T_{coh} \sim 40\text{K}$ is the temperature below which the electrical resistivity exhibits the T^2 behavior expected for a Fermi liquid. The low temperature optical conductivity of YbAl_3 exhibits[9] both a very narrow Drude resonance and a mid-infrared peak that is associated with optical transitions across the renormalized hybridization gap. The Drude peak begins to broaden and the mid-IR peak begins to be suppressed above 40K. Hence, the optical conductivity indicates that 40K is the temperature scale for full establishment of the renormalized band structure. In a $1/N_J$ -expansion treatment[10] of the Anderson lattice for $N_J = 2J + 1 = 6$, the coherence temperature (defined here also as the temperature where the renormalized Fermi liquid is fully established) was found to satisfy $T_{coh} \approx T_K/10$, which is approximately true for YbAl_3 . In this treatment, a low temperature anomaly in the susceptibility was predicted for $T < T_{coh}$ when the total electron density $n_c + n_f$ was set to a value (1.9) that is close to the value appropriate for a Kondo insulator, i.e. in the limit of low conduction hole density. A recent slave Boson treatment[11] of the

Anderson lattice in the limit of low conduction *electron* density also shows anomalies in the susceptibility and specific heat for $T < T_{coh}$. Hence our recent experimental results for YbAl₃ [4] which show both a susceptibility anomaly and a specific heat anomaly (Fig. 1, inset) below 40K may be explained by the Anderson lattice in the limit of low conduction electron or hole density.

The results reported here show that above a transition field $B^* \sim 40\text{T}$ the dHvA masses for key branches of Fermi surface decrease by approximately a factor of two. The specific heat anomaly (Fig. 1 inset) is consistent with this, in that the low temperature value is twice as large as the value extrapolated from higher temperature; and we predict that the specific heat coefficient will decrease by a factor of two above 40T. As discussed above, we expect the transition field for polarization of the $4f$ level in the Anderson lattice to satisfy $gJ\mu_B B_K \approx k_B T_K$ [7, 8, 12]. For YbAl₃ where $g = 8/7$, $J = 7/2$ and $T_K = 670\text{K}$, this formula gives $B_K = 250\text{K}$, much larger than the observed value of B^* . The theory also predicts that the susceptibility will increase as the field increases in the vicinity of B_K ; the $4f$ polarization can be thought of as a continuous metamagnetic transition [12]. However, the susceptibility of YbAl₃ *decreases* at B^* . Finally, for systems such as CeRu₂Si₂ where the metamagnetic transition is observed experimentally, the Fermi surface alters at the transition because the polarization corresponds to a localization of the $4f$ electron which causes it to drop out of the Fermi volume [13]. For YbAl₃, however, the transition has only a small effect on the Fermi surface geometry, with most frequencies unchanged but with a 25% increase in the frequency of the β branch along $\langle 111 \rangle$ which is suggestive of an *increase* in the Fermi volume. These facts suggest that the reduction of the masses is not connected with a simple polarization of the $4f$ level.

The transition field energy *is*, however, of order of $k_B T_{coh}$, which suggests that the field dependence of the masses is intimately related to the existence of the low temperature anomalies. For $B > B^*$ the susceptibility anomaly is suppressed and the temperature dependence becomes qualitatively similar to that of an Anderson impurity [4]. The effective masses reduce to values that are still moderately large, comparable indeed to those of CeSn₃ [2], without much change in the Fermi surface geometry. It is as though the transition turns the compound into a non-anomalous intermediate valence compound, with moderately renormalized bands, but without $4f$ polarization. It remains to be seen whether the theory of the Anderson lattice can explain these effects and clarify the difference between

anomalous and non-anomalous IV compounds.

Work by T. E. in the U.S. was supported by the Research Abroad Program of the Japanese Ministry of Education; work in Japan was supported in part by the Inoue Science Promotion Foundation and in part by Corning Japan. Work at UNLV was supported by DOE EPSCoR-State/National Laboratory Partnership Award DE-FG02-00ER45835 and DOE Cooperative Agreement DE-FC08-98NV1341. Work by J.L. in Japan was supported by the Japanese Society for the Promotion of Science; work at UC Irvine was supported by UC/DRD funds provided by the University of California for the conduct of discretionary research by the Los Alamos National Laboratory and by the UC/LANL Personnel Assignment Program. Work at the National High Magnetic Field Laboratory, Los Alamos Facility, was performed under the auspices of the National Science Foundation, the State of Florida and the Department of Energy.

* Electronic address: jmlawren@uci.edu

- [1] A. Hasegawa and H. Yamagami, Progress of Theoretical Physics Supplement **108**, 27 (1992).
- [2] S. Tanaka, H. Harima and A. Yanase, Journ. Mag. Mat. **177-181**, 329 (1998).
- [3] T. Ebihara, Y. Inada, M. Murakawa, S. Uji, C. Terakura, T. Terashima, E. Yamamoto, Y. Haga, Y. Onuki and H. Harima, Journ. Phys. Soc. Japan **69**, 895 (2000).
- [4] A. L. Cornelius, J. M. Lawrence, T. Ebihara, P.S. Riseborough, C. H. Booth, M. F. Hundley, P. G. Pagliuso, J. L. Sarrao, J. D. Thompson, M. H. Jung, A. H. Lacerda and G. H. Kwei, Phys. Rev. Lett. **88**, 117201 (2002).
- [5] V. N. Antonov, M. Galli, F. Marabelli, A. N. Yaresko, A. Ya. Perlov and E. Bauer, Phys. Rev. B **62**, 1742 (2000).
- [6] N. Harrison, P. Meeson, P.-A. Probst and M. Springford, J. Phys.: Condens. Matter **5**, 7435 (1993).
- [7] P. Schlottmann, Phys. Rev. B **35**, 5279 (1987).
- [8] A. Wasserman, M. Springford and A. C. Hewson, J. Phys.: Condens. Matter **1**, 2669 (1989).
- [9] H. Okamura, T. Ebihara and T. Nanba, Acta Physica Polonica, to be published (cond-mat/0208006); and unpublished data.
- [10] Y. Ōno, T. Matsuura and Y. Kuroda, Journ. Phys. Soc. Japan **60**, 3475 (1991).

- [11] S. Burdin, A. Georges and D. R. Grempel, Phys. Rev. Lett. **85**, 1048 (2000).
- [12] Y. Ōno, Journ. Phys. Soc. Japan **65**, 19 (1996).
- [13] Y. Ōnuki, R. Settai and H. Aoki, Physica B **223&224**, 141 (1996).

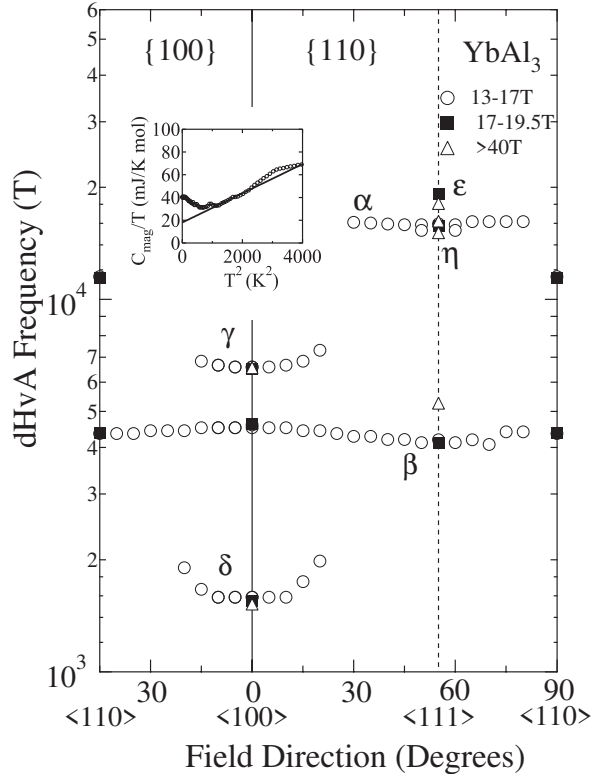


FIG. 1: The de Haas-van Alphen frequencies of YbAl_3 as a function of angle with respect to the high symmetry directions. The different symbols correspond to different field ranges for the measurement. The inset shows the coefficient C_{mag}/T of the magnetic contribution to the specific heat as a function of T^2 to demonstrate that the low field value is enhanced by a factor of two with respect to the value extrapolated from higher temperature.

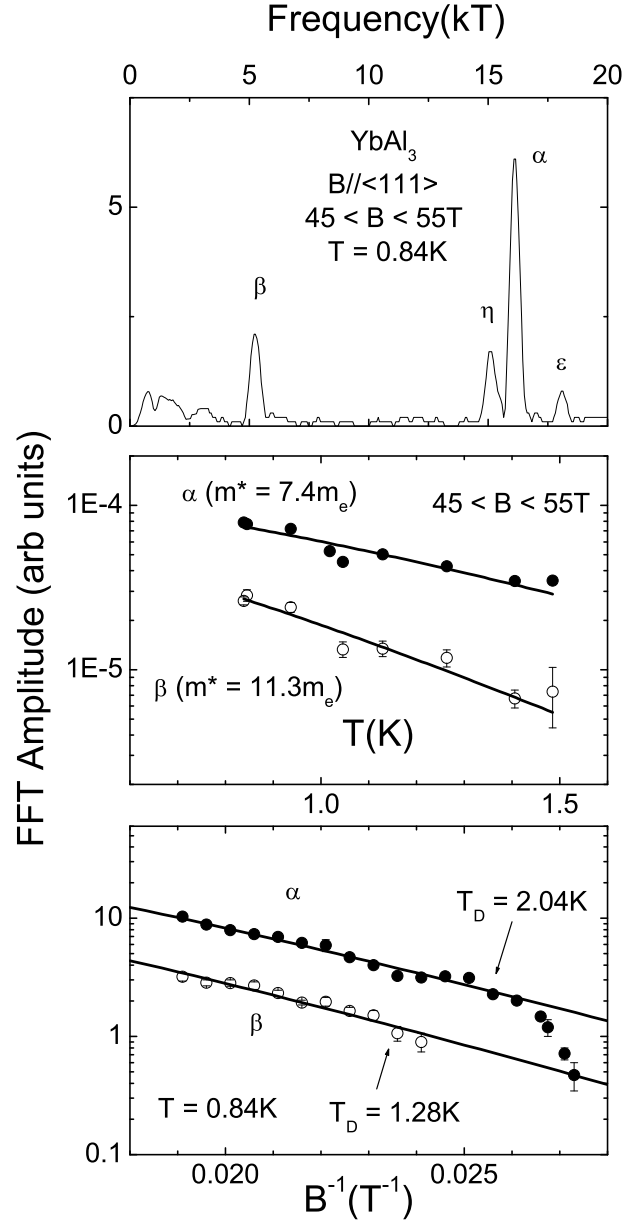


FIG. 2: a) The fast Fourier transform of the de Haas-van Alphen spectrum at 0.84K for field along the $\langle 111 \rangle$ direction for fields in the range $45 \leq B \leq 55\text{T}$. b) A mass plot and c) a Dingle plot for the α and β branches for field along $\langle 111 \rangle$. (See text for the fitting function.)

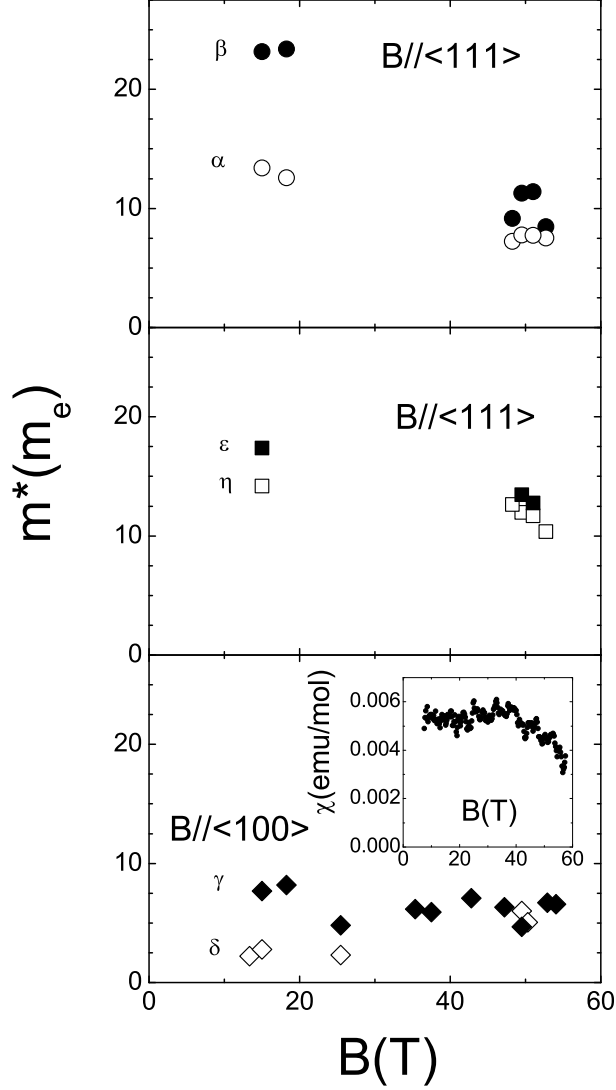


FIG. 3: The dHvA masses in units of the free electron mass m_e for different branches of the Fermi surface of YbAl_3 as a function of magnetic field for a) and b) field along the $\langle 111 \rangle$ direction and c) field along the $\langle 100 \rangle$ direction. A large reduction of the α and β branches is observed at high field. Inset: The field dependence of the magnetic susceptibility, showing that $\chi(B)$ decreases for $B > 40\text{T}$.